Nanosurface Chemistry on Size-Selected Silicon Clusters

MARTIN F. JARROLD

Studies of the chemistry that occurs on the nanosurfaces of size-selected silicon clusters reveal a number of fascinating qualitative similarities to the behavior of bulk surfaces. However, silicon clusters containing up to 70 atoms appear to be much less reactive than bulk silicon surfaces. This unexpected result suggests that these large silicon clusters are not just small crystals of bulk silicon, but have much more compact geometric structures.

AN ATOMIC CLUSTER IS A SMALL PIECE OF MATERIAL containing between three and several hundred atoms. Investigating the physical and chemical properties of atomic clusters of metallic, nonmetallic, and semiconductor elements is currently one of the most active frontiers in chemistry and physics (*1*). Small atomic clusters have properties very different from those of the bulk material because of their small physical size, and there is particular interest in determining how many atoms are required for bulk-like behavior to emerge. In some cases this number appears to be remarkably small. For example, the electronic properties of alkali metal clusters containing as few as eight atoms can be explained by a free electron model (*2*) and the optical absorption spectrum is dominated by a narrow feature which can be attributed to a surface plasma resonance (*3*). Along with the interest in the physical properties of atomic clusters, there is a corresponding interest in the chemical properties (*4*). The nanosurfaces of small atomic clusters may show chemical properties quite different from those of the bulk material. Given the large surface-to-volume ratio and the large step and defect density we might expect small atomic clusters to be highly reactive. Some clusters may be special, either particularly reactive or particularly inert, but for a sufficiently large cluster, bulk-like behavior is expected to emerge. In addition to the fundamental interest in their chemical properties, studies of chemistry that occurs on the nanosurfaces of atomic clusters provide a new way to study surface processes. These studies may generate further insight into the fundamental steps that make up the complicated chemical processes that take place on surfaces. This article will focus on recent studies of the chemical properties of silicon clusters containing up to 70 atoms. Silicon is of paramount importance in the multibillion dollar microelectronics industry, and if current miniaturization trends continue the minimum structure size will approach the scale of these small clusters in a couple of decades. Because structure is important in chemistry, I will start by briefly considering what is known about the geometric structure of silicon clusters.

Structure of Small Silicon Clusters

The structure of molecules has traditionally been determined by molecular spectroscopy whereas diffraction-based methods are used for bulk materials. Clusters with 10 to 70 atoms lie in the awkward size regime where both approaches have severe problems. It is also difficult to generate the large density of size-selected silicon clusters required for these methods. So there is not yet any direct experimental information on the structure of clusters in this size regime. The natural way to start thinking about the structure of atomic clusters is as small pieces of the bulk lattice. At room temperature and atmospheric pressure bulk silicon has a diamond-like structure with tetrahedrally coordinated silicon atoms. Several structures are possible for a Si_{10} cluster (Fig. 1). The one on the left side of the figure is a bulk fragment (a cluster with this structure can be plucked from the bulk material). However, high level ab initio theoretical calculations for Si_{10} suggest that this structure is not very stable (*5*). A quick glance at Fig. 1 reveals why. Silicon likes to be tetrahedrally coordinated, but the silicon atoms in the structure on the left side of Fig. 1 are bound to only two or three other atoms. Thus there are a large number of dangling bonds. Dangling bonds also occur on the clean surfaces of bulk silicon and the energy gained by using these dangling bonds to form bonds to other silicon atoms provides the motivation for surface reconstruction. For example, the (7×7) reconstruction of the Si(111) surface reduces the number of dan-

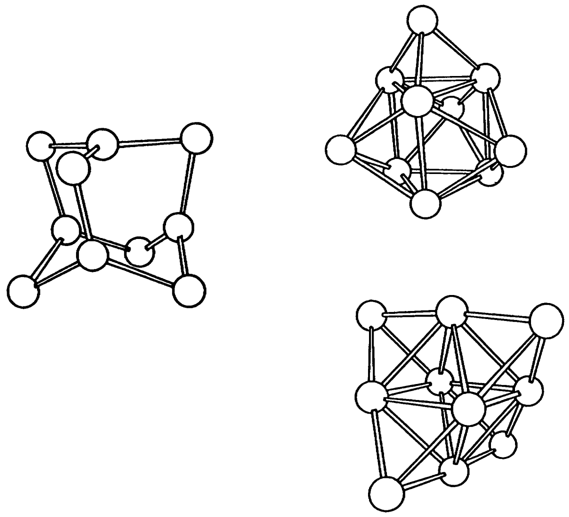

Fig. 1. Possible structures for Si_{10}. The one on the left is a bulk fragment. The more compact structures on the right are around 5 eV more stable than the bulk fragment. Both of these structures probably exist. For a more complete discussion of these structures and possible structures for other cluster sizes see Raghavachari (*6*).

The author is at AT&T Bell Laboratories, Murray Hill, NJ 07974.

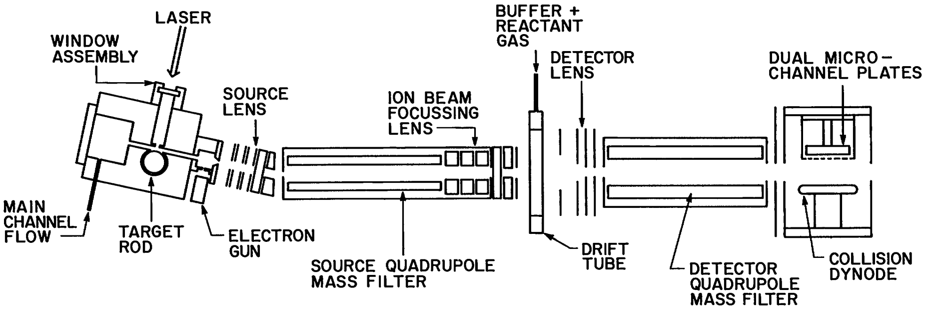

Fig. 2. Schematic diagram of experimental apparatus used to investigate the chemical properties of size-selected silicon cluster ions.

gling bonds by over 60%. According to the theoretical calculations Si_{10} also reconstructs to reduce the number of dangling bonds. The two lowest energy structures for Si_{10}, determined from theoretical calculations, are shown on the right side of Fig. 1 (*6*). These structures are sufficiently close in energy in the calculations that it is not possible to say with complete confidence which is the most stable. It will be shown below that both structures probably exist. The structures shown on the right in Fig. 1 are very different from the diamond structure of bulk silicon. They are more close-packed and some of the atoms have coordination numbers greater than four. In fact these structures appear to be more closely related to the high-pressure metallic phases of bulk silicon (such as the β-tin structure) than to the diamond structure. The energy gained by reconstructing to the more close-packed structures is, according to the theoretical calculations, ~5.0 eV (*6*). While this is substantial, it is apparent from Fig. 1 that the number of bonds has increased from 12 in the bulk fragment to 24 in the more close-packed structures. Thus these extra bonds resulting from reconstruction are relatively weak. The reason for this is strain. Reconstruction takes many of the silicon atoms away from the favored tetrahedral configuration.

Sophisticated calculations like those described above for Si_{10} cannot yet be performed for much larger clusters, so little is known about their structures. Furthermore, the cluster size regime where the diamond structure becomes favorable compared to the more close-packed structures is not known.

Experimental Methods

A schematic diagram of the experimental apparatus used to investigate the chemical reactivity of size-selected silicon clusters is shown in Fig. 2 (*7*). The silicon cluster ions are generated by pulsed laser vaporization (*8*). A pulsed laser is focused onto a silicon rod, vaporizing some silicon as a plume of atoms above the rod. The vaporized silicon atoms are entrained and cooled in a stream of helium, and clusters grow as the vaporized material is carried through the source. After formation, the clusters undergo $>10^5$ collisions with the buffer gas which ensures that they are at room temperature when they exit the source. Ions are also formed in the laser vaporization process and a significant fraction of the clusters which leave the source are ionized. After leaving the source the cluster ions are focused into a quadrupole mass spectrometer. A portion of a mass spectrum of silicon cluster ions generated by pulsed laser vaporization is shown in Fig. 3A. The peaks in the mass spectrum are around 8 atomic mass units wide because of the isotope distribution of silicon. Laser vaporization generates a broad distribution of cluster sizes, but since the clusters are charged mass spectrometry can be used to select a specific cluster size for detailed study. Thus it is possible to generate a beam of single-sized clusters. The mass spectrum of a beam of size-selected Si_{40}^+ clusters is shown in Fig. 3B. The amount of Si_{40}^+ present, however, is extremely small: only around 10^4 to 10^5 clusters per second.

To study their chemical reactivity, the beam of size-selected clusters is injected at low energy into a miniature drift tube containing the chemical reagent diluted in neon buffer gas. The clusters undergo chemical reactions as they drift across the drift tube under the influence of a weak electric field. The drift field is sufficiently weak that any chemical reactions that occur take place under thermal energy conditions at the temperature of the drift tube walls. The temperature of the drift tube can be adjusted from 77 K to 700 K. At the other end of the drift tube, a small fraction of the product ions and unreacted cluster ions exit through a small aperture, they are subsequently mass-analyzed by a second quadrupole mass spectrometer, and then detected. Figure 3C shows the mass spectrum recorded by scanning the second quadrupole for the reaction between Si_{40}^+ and ethylene (C_2H_4).

Reactions with Ethylene: Evidence for Isomers

As can be seen from the spectrum shown in Fig. 3C, the products from the reaction between Si_{40}^+ and ethylene arise from adsorption of ethylene molecules onto the cluster surface. More than one ethylene molecule adsorbs to give a range of $Si_{40}(C_2H_4)_m^+$ products (*7, 9*). All the other clusters react in the same way (except for Si_3^+ which dehydrogenates ethylene to yield $Si_3C_2H_2^+$). Under our

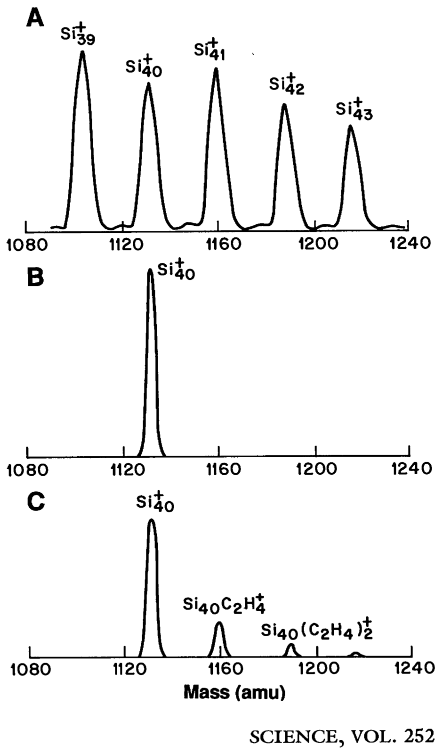

Fig. 3. Mass spectra of silicon cluster ions generated by pulsed laser vaporization. (**A**) Before size selection. (**B**) After selection of Si_{40}^+. (**C**) After reaction of size-selected Si_{40}^+ with ethylene. The small peaks between the silicon cluster peaks in (A) arise from oxygen contamination to give Si_nO^+ species. This contamination is removed by size selection. The widths of the peaks in (A) are ~8 atomic mass units wide because of the isotope distribution of silicon. The isotope distribution of size-selected Si_{40}^+ in (B) has been narrowed down to ~4 atomic mass units wide.

experimental conditions, the reactions are expected to follow pseudo–first order kinetics, and the rate constant k_r for the addition of the first ethylene is given by:

$$\ln\frac{I}{I_0} = -k_r n[C_2H_4]t \qquad (1)$$

where I_0 is the initial Si_n^+ intensity, I is the final Si_n^+ intensity, $n[C_2H_4]$ is the ethylene number density, and t is the average time the clusters spend in the drift tube. According to Eq. 1, a plot of $\ln(I/I_0)$ against either $n[C_2H_4]$ or t should be a straight line with a slope proportional to k_r. Figure 4 shows a plot of $\ln(I/I_0)$ against ethylene pressure (which is proportional to $n[C_2H_4]$) for Si_{26}^+. It is clear that the experimental data is far from the expected straight line. There appear to be two different pressure regimes. In the first regime (with ethylene pressures less than 0.5 mtorr) the clusters react away very rapidly. In the second regime they react much more slowly. The explanation for these two regimes is that there are two different types of Si_{26}^+ clusters: a more reactive form and a less reactive form. These different forms of the Si_{26}^+ cluster are structural isomers, they have different geometric structures (*7, 9*). Similar experiments performed for the other clusters have demonstrated that structural isomers exist for virtually all silicon clusters with more that eight atoms. Unfortunately, these experimental results cannot provide detailed information about the structures of the isomers. However, in the case of Si_{10}^+, which was discussed above, we have a pretty good idea from the theoretical calculations what the isomers look like (see Fig. 1).

Isomerization and Annealing

The presence of at least two different structures for a Si_{26}^+ cluster is not surprising. Amorphous silicon, a noncrystalline material with no long-range order, can be formed by either rapid quenching of the liquid or by evaporation. Amorphous silicon can be crystallized by annealing. If the clusters were amorphous there would be numerous structural isomers present. So the fact that we appear to see only two different isomer populations suggests that a considerable amount of annealing occurs as the clusters grow in the source. The energy released as a silicon atom binds to a growing cluster (~4 eV) presumably causes this annealing. It is possible to anneal the clusters further by heating them and then cooling. Smalley and co-workers have shown that laser annealing of silicon clusters can influence their reactivity (*10*). In our experiments collisional annealing is used (*9, 11*). The clusters are injected at high kinetic energy (50 to 200 eV) into the drift tube where they are heated by collisions with the buffer gas. After the clusters' kinetic energy is thermalized, they are cooled by further collisions with the buffer gas. This heating and cooling cycle anneals the clusters. If the injection energy is sufficiently large it is possible to heat the clusters to the point where they start to fall apart. When bulk silicon is heated, atoms evaporate from the surface. Silicon clusters behave very differently; instead of evaporating individual atoms, units of six or ten atoms evaporate (*12, 13*). Thus, for example, Si_{60}^+ dissociates to yield mainly Si_{54}^+ and Si_6 (*13*). The reason for this behavior is not completely understood. Theoretical calculations indicate that Si_6 and Si_{10} are particularly stable (*6*), but it still should be much easier to evaporate an atom from the cluster than a large Si_6 or Si_{10} fragment.

Figure 4 shows a comparison of the reactivity of annealed Si_{26}^+ clusters with the behavior of unannealed clusters coming directly from the source (*11*). Annealing the clusters does indeed appear to have altered the relative abundance of the more reactive and less reactive isomers. From the data shown in Fig. 4 it appears that the relative abundance of the more reactive isomer has increased from ~18% for the unannealed clusters to ~28% for the annealed clusters. These results suggest that the reactive isomer is slightly more stable than the unreactive isomer. This conclusion may appear to be counterintuitive, but there is no reason to expect a correlation between thermodynamic stability and chemical reactivity. My co-workers and I have performed these experiments for a number of different cluster sizes and annealing does not cause a systematic change in the reactivity. For some clusters (like Si_{26}^+ above) annealing makes the cluster more reactive; but for others, annealing makes the cluster less reactive.

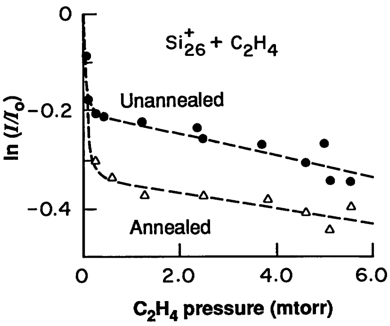

Fig. 4. Plot of $\ln(I/I_0)$ versus ethylene pressure for Si_{26}^+. The figure shows results for annealed and unannealed clusters. Note that there appear to be two components present. One component reacts away with pressures less than 0.5 mtorr. The other component is much more inert. Annealing the clusters (with an injection energy of 50 eV) alters the relative abundance of the reactive and unreactive isomers.

Having firmly established the existence of structural isomers and shown that it is possible to anneal them, the next challenge is to determine how much energy is required to interconvert the different isomers. Amorphous silicon crystallizes at around 900 K and it seems unlikely that a temperature much higher than this should be required to anneal the clusters. For one cluster, however, it appears that the isomers interconvert at a much lower temperature. Experimental results for Si_{20}^+ suggest that this cluster interconverts between reactive and unreactive isomers on a millisecond time scale at room temperature (*9*). Si_{20}^+ is exceptional in this regard, however, and the isomers of the other clusters, including Si_{26}^+ discussed above, do not appear to interconvert so readily, though the annealing temperatures have not yet been determined.

The kinetics of the reactions of the silicon clusters with other reagents discussed below do not appear to be as sensitive to the presence of structural isomers as the reactions with ethylene. Studies of the reactions of ethylene with bulk silicon surfaces show that ethylene adsorbs molecularly in a di-σ bonded state (*14*). It seems likely that this unique bonding configuration could give rise to the observed sensitivity to the presence of structural isomers because adsorption of ethylene probably requires a particular type of site on the cluster.

Reactions with Oxygen and Water: Etching Versus Chemisorption

Two product channels are observed in the reactions between the silicon clusters and oxygen (O_2) (*15*). For clusters with less than 30 atoms the etching reaction

$$Si_n^+ + O_2 \rightarrow Si_{n-2}^+ + 2SiO \qquad (2)$$

dominates. Here each reaction of an oxygen molecule with the silicon cluster results in the loss of two silicon atoms as two SiO molecules. This reaction will ultimately etch the cluster, two atoms at a time, all the way down to Si_2^+ or Si^+ (*16*). For clusters with more than 35 atoms the chemisorption reaction

$$Si_n^+ + O_2 \rightarrow Si_nO_2^+ \qquad (3)$$

dominates. At the transition between etching and chemisorption (that occurs for clusters with 30 to 35 atoms) product ions arising from the loss of a single SiO molecule are observed. Exposure of clean bulk silicon surfaces to oxygen at room temperature results in dissociative chemisorption (*17–20*). However, if the oxidized silicon surface is heated to ~1000 K, SiO desorbs from the surface. So the clusters appear to be behaving like the bulk surface. There is a simple explanation for the switch from etching to chemisorption that occurs for clusters with 30 to 35 atoms. Oxidation of the clusters is a very exothermic process resulting in a hot $Si_nO_2^+$ product. The small clusters have fewer internal degrees of freedom so when they are oxidized they get hotter and evaporate SiO molecules before they can be cooled by collisions with the buffer gas. This explanation is confirmed by studies of the oxidation of size-selected silicon clusters deposited on amorphous carbon substrates (*21*). The deposited clusters are in good thermal contact with the substrate and when they are oxidized the exothermicity is rapidly conducted away. No etching is observed for deposited clusters even as small as Si_{10}.

Unlike the reactions with oxygen, the reactions with water (D_2O) result in the formation of a series of $Si_n(D_2O)_m^+$ products for all cluster sizes (*22, 23*). No etching reactions were observed. The available evidence suggests that adsorption of D_2O on to the silicon clusters involves dissociative chemisorption to yield −D and −OD bound separately to the cluster surface. Similar behavior is observed on bulk silicon surfaces (*24–27*).

Sticking Probabilities for Oxygen and Water: Comparison with the Bulk

The reactions of oxygen and water do not appear to be as sensitive to the presence of structural isomers as the reactions with ethylene. Thus plots of $\ln(I/I_0)$ against reagent pressure for these reactions are in most cases close to linear, and the reaction kinetics can be described by a single rate constant. Plots of the rate constants obtained for the reactions of Si_n^+ (n = 10–65) with oxygen and water are shown in Fig. 5 (*15, 23*). Note that these rate constants are for the addition of the first reagent molecule to the cluster (or the first etching reaction). As can be seen from Fig. 5, there are large variations in the reactivity of the smaller clusters. The variations diminish with increasing cluster size, and for clusters with more than 40 atoms the reactivity changes only slightly with the number of atoms in the cluster. A number of the smaller clusters appear to be particularly unreactive. With oxygen the unreactive clusters are those with 13 and 14 atoms. Clusters with 11, 13, 14, 19, and 23 atoms are particularly unreactive toward water. Clusters with 13, 14, and 23 atoms are also particularly unreactive toward ethylene (*7, 9*). It is clear that as the unreactive clusters are listed the same numbers keep appearing. In particular, Si_{13}^+ is the least reactive cluster with ethylene, oxygen, and water.

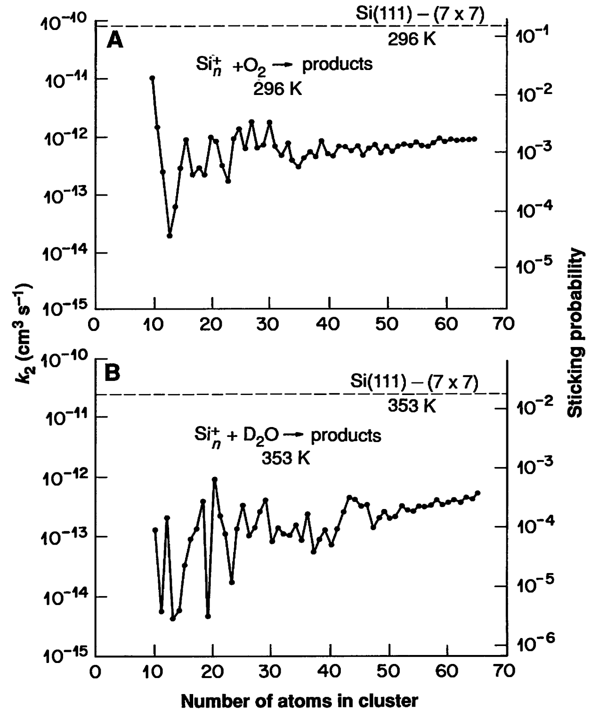

Fig. 5. Absolute rate constants for the reactions of silicon cluster ions with (**A**) oxygen [data from (*15*)] and (**B**) heavy water [data from (*23*)]. The dashed lines show the reactivity of Si(111)-(7×7) (*17, 26*).

A 13-atom cluster is unique because several very symmetric geometric structures are possible. Chelikowsky and Phillips (*28*) have used an interatomic potential to model silicon clusters with up to 25 atoms. According to their model some clusters show an icosahedral growth sequence. Thus Si_{13} is predicted to be an icosahedron (with a 1-5-1-5-1 layer structure). Si_{19} is predicted to be a double icosahedron obtained by capping Si_{13} with a six-atom cap (to give a 1-5-1-5-1-5-1 layer structure). The next "magic number" is at n = 23 which is obtained by adding another cap with edge sharing. The icosahedral growth sequence n = 13, 19, 23, 26, . . . , 55, has previously been found in rare gas clusters (*29*). As noted by Chelikowsky and Phillips (*28*) this provides a plausible way to account for most of the unreactive clusters. However, it does not account for all of them. In particular, Si_{14}^+ is not a "magic number" in this sequence, but it is almost as unreactive as Si_{13}^+. So there is not yet a completely satisfactory explanation for why some of the smaller clusters are particularly unreactive.

The reactivity of surfaces is usually expressed in terms of an initial sticking coefficient. This represents the probability that a particular reaction (dissociative chemisorption in this case) occurs on a clean surface. The rate constants shown in Fig. 5 can be expressed in terms of a sticking probability with the equation

$$S_0 = \frac{k_r}{k_c} \qquad (4)$$

where k_r is the measured rate constant for the reaction and k_c is the calculated collision rate. The collision rate is calculated with simple models appropriate for ion-molecule reactions (*30*). The scale on the right side of Fig. 5 shows the sticking probability. The sticking probability of oxygen on the larger silicon clusters (n = 40–65) is around 10^{-3}. The sticking probability of water is even lower, it is in the 10^{-4} range. Clearly, these are not very efficient reactions.

The cluster sticking probabilities can be compared with the initial sticking coefficients on bulk silicon surfaces. The dashed lines in Fig. 5 shows the initial sticking coefficients for oxygen (*17, 18*) and water (*24, 26*) on Si(111)-(7×7), the lowest energy surface of bulk silicon. The clusters appear to be around two orders of magnitude less reactive than the bulk surface.

Studying reactions on bulk surfaces is exceedingly difficult and there is often a wide variation in the initial sticking coefficients reported by different groups (*17–20, 24–27*). One problem with studying surface reactions is that the surface can become contaminated. This is not a problem with the cluster studies reported here because, for a typical cluster, the time from formation to detection is only several milliseconds, and any contamination would be apparent from the mass spectrum of the size-selected clusters. The reactions of oxygen and water with Si(111)-(7×7) have recently been studied by several groups and their results are in good agreement (*17, 18, 24, 26*). However, less is known about the other surfaces of bulk silicon. It appears that sticking coefficients for oxygen on Si(100), Si(110), and sputtered Si(111) are within a factor of 4 of that for Si(111)-(7×7) (*19*). A sticking coefficient of

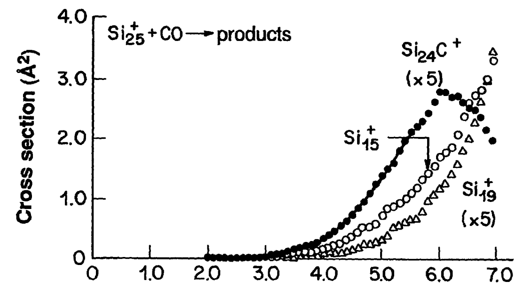

Fig. 6. Cross sections measured using the low energy ion beam configuration for the reactions of Si_{25}^+ with carbon monoxide [data from (*32*)]. Si_{15}^+ arises from collision-induced dissociation. The other products arise from dissociative chemisorption of carbon monoxide on the Si_{25}^+ cluster. The substantial kinetic energy threshold associated with dissociative chemisorption shows that there is a large activation barrier for breaking the C-O bond.

2×10^{-4} has been reported for atomically flat Si(111)-(2×1), but the sticking coefficient on this surface was found to increase exponentially with step density reaching a value of 0.1 when ~15% of the atoms are at steps (*20*). Less is known about the interaction of water with bulk silicon. Si(100)-(2×1) has been the most extensively studied surface. On this surface the sticking coefficient is ~1 at room temperature (*27*)—around four orders of magnitude larger than on the clusters. The sticking coefficient of water on Si(111)-(7×7) shown in Fig. 5 by the dashed line was obtained on a silicon crystal cut at 4° to the (111) plane. Measurements performed by George and co-workers at Stanford University in the last few months suggest that a completely flat Si(111)-(7×7) surface is over an order of magnitude less reactive (*26*). This result implies that steps on the Si(111)-(7×7) surface play an important role in promoting dissociative chemisorption of water.

Molecular Versus Dissociative Chemisorption

As described above the interaction of oxygen and water with silicon clusters and bulk silicon results in dissociative chemisorption. Chemisorption is not always dissociative. Carbon monoxide (CO) is an example of a reagent which often undergoes molecular adsorption on metal surfaces. Carbon monoxide does not react with bulk silicon at room temperature, and it does not react with the silicon clusters at room temperature either (*31*). One of the advantages of working with ions is that their energies can readily be controlled. Figure 6 shows some results obtained with a low energy ion beam experiment to study the reaction between Si_{25}^+ and carbon monoxide (*32*). For the low energy ion beam experiments the drift cell is replaced by a gas cell containing a low pressure of the reagent. With this configuration the reactions occur under single collision conditions with a well-defined collision energy. The figure shows a plot of the cross sections for forming the observed product ions against the center of mass collision energy. Three product ions are observed: $Si_{24}C^+$, Si_{19}^+, and Si_{15}^+. The Si_{15}^+ product does not arise from a chemical reaction, it arises from collision-induced dissociation. As described above, silicon clusters dissociate by loss of six or ten atom units. Si_{25}^+ dissociates almost exclusively by loss of Si_{10} to give Si_{15}^+. The other product ions result from dissociative chemisorption of carbon monoxide. The $Si_{24}C^+$ product arises from loss of the now familiar SiO molecule from $Si_{25}CO^+$, the product of dissociative chemisorption which is not directly observed in these experiments. Si_{19}^+ results from the further loss of Si_5C from $Si_{24}C^+$ (the Si_{19}^+ does not result from simple collision-induced loss of Si_6 from Si_{25}^+ because, as noted above, collision-induced dissociation of Si_{25}^+ results almost exclusively in loss of Si_{10} to give Si_{15}^+). As can be seen from the figure there are kinetic energy thresholds associated with the reactions. The threshold for $Si_{24}C^+$ can be attributed to the activation barrier for dissociative chemisorption of carbon monoxide on Si_{25}^+. A detailed analysis of the threshold region yields an activation barrier of ~3.1 eV. The large activation barrier associated with breaking the C-O bond clearly explains why dissociative chemisorption does not occur at room temperature.

While carbon monoxide does not react with the silicon clusters at room temperature, if the temperature of the drift tube is lowered to 77 K a series of $Si_n(CO)_m^+$ products are observed (*31*). These products, however, do not arise from dissociative chemisorption, they arise from molecular adsorption where the carbon monoxide is bound as a molecule to the cluster. From studies of the equilibrium

$$Si_n(CO)_{m-1}^+ + CO \rightleftharpoons Si_n(CO)_m^+ \qquad (5)$$

as a function of temperature it is possible to determine values for the enthalpy change (ΔH^0) and entropy change (ΔS^0) associated with binding a carbon monoxide molecule to the cluster. These results show that carbon monoxide is very weakly bound to the clusters as a molecule (the binding energies are ~0.1 eV). Furthermore, the small values found for the entropy change suggest that the carbon monoxide molecule moves freely over the surface of the cluster in a miniature version of surface diffusion. The high mobility of carbon monoxide over the cluster surface arises because of the low binding energy.

A slightly different picture has emerged from studies of the reactions of the silicon cluster ions with ammonia. Ammonia reacts readily with bulk silicon surfaces. The sticking coefficient, at room temperature, on both Si(111)-(7×7) and Si(100)-(2×1) is close to one (*34–36*). The most recent results indicate that dissociative chemisorption occurs in a self-limiting reaction which ceases when all the surface dangling bonds are saturated. Avouris and co-workers have shown that clean Si(100)-(2×1) can dissociate ammonia at temperatures as low as 90 K (*35*). Studies of the reactions of the silicon clusters at room temperature reveal that they also appear to be very reactive toward ammonia. The reaction results in the formation of a series of $Si_n(ND_3)_m^+$ products and it occurs at close to the collision rate (sticking probability ~1) (*33*). However, as the temperature is increased a significant difference between the behavior of the clusters and the bulk surface becomes apparent. If a bulk silicon surface is exposed to ammonia and then heated, H_2 desorbs at around 800 K and Si_2N desorbs at around 1350 K (*34*). But as the temperature of the drift tube is increased intact ammonia molecules desorb from the $Si_n(ND_3)_m^+$ products. At temperatures around 400 K an equilibrium,

$$Si_n^+ + ND_3 \rightleftharpoons Si_nND_3^+ \qquad (6)$$

can be established. From measurements of the equilibrium constants as a function of temperature, binding energies of ammonia to the silicon clusters were determined (*13*). The binding energies are ~1 eV. This is much larger than the binding energies of molecular carbon monoxide to the clusters, but a binding energy of ~1 eV is also much too small to be accounted for by dissociative chemisorption. If dissociative chemisorption occurred the binding energy of ammonia to the silicon clusters would be ~3 eV. Thus it appears that, unlike the bulk surface, at close to room temperature the reaction between the silicon clusters and ammonia results in molecular adsorption and not dissociative chemisorption. The relatively large binding energy between molecular ammonia and the silicon clusters is not unexpected. Ammonia is known to be a strong Lewis base and it forms strongly bound donor-acceptor complexes with a number of different reagents. For example, the donor-acceptor complex between SiH_2 and ammonia is bound by 1.1 eV (*37*). What is surprising, however, is that the silicon clusters apparently cannot dissociate ammonia even though bulk silicon surfaces do at temperatures as low as 90 K.

As the temperature of the drift tube is raised, the equilibrium process represented by Eq. 6 is pushed over to the left and less of the molecularly adsorbed product is formed. At temperatures above 500 K another process, resulting in ammonia more strongly bound to the cluster surface, becomes important. This process presumably results in dissociative chemisorption of ammonia (*13*). Both molecular adsorption and dissociative chemisorption yield $Si_nND_3^+$ products which cannot be distinguished by simple mass spectrometry alone. However, it was possible to distinguish the different processes by careful measurements where both the reaction time and reagent pressure were varied. At temperatures between 500 K and 700 K products arising from both molecular adsorption and dissociative chemisorption are observed. But at 700 K the amount of molecularly adsorbed product present is extremely small and essentially all the observed product results from dissociative chemisorption. Figure 7 shows a plot of the rate constants for dissociative chemisorption of ammonia at 700 K for clusters with 30 to 70 atoms. The scale on the right shows a sticking probability scale. The sticking probabilities for the clusters are extremely small, between 10^{-3} and 10^{-5}. For comparison the initial sticking coefficient on bulk Si(111)-(7×7) is around 0.1 at 700 K (*34*). Again it appears that the clusters are much less reactive than the bulk surface.

The rate constants for clusters with 30 to 50 atoms show substantial variations with cluster size (see Fig. 7). Si_{45}^+ is noticeably less reactive than its neighbors. Smalley and co-workers have investigated the reactions of silicon cluster ions in this size regime with ammonia and found Si_{33}^+, Si_{39}^+, and Si_{45}^+ to be between one and two orders of magnitude less reactive than their neighbors at room temperature (*38*). As described above, at room temperature we find that all the clusters react with ammonia at close to the collision rate to generate a product where ammonia is bound as an intact molecule to the cluster surface. Smalley and co-workers used Fourier transform ion cyclotron resonance (FT-ICR) in their studies. In the FT-ICR experiments the pressures are much lower, and the reaction times correspondingly longer than in the drift tube experiments described above. While the origin of the difference between the results obtained by the two experimental techniques has not yet been completely resolved, it appears that the molecular adsorption process observed at room temperature in the drift tube experiments does not occur with the same efficiency in the lower pressure FT-ICR experiments.

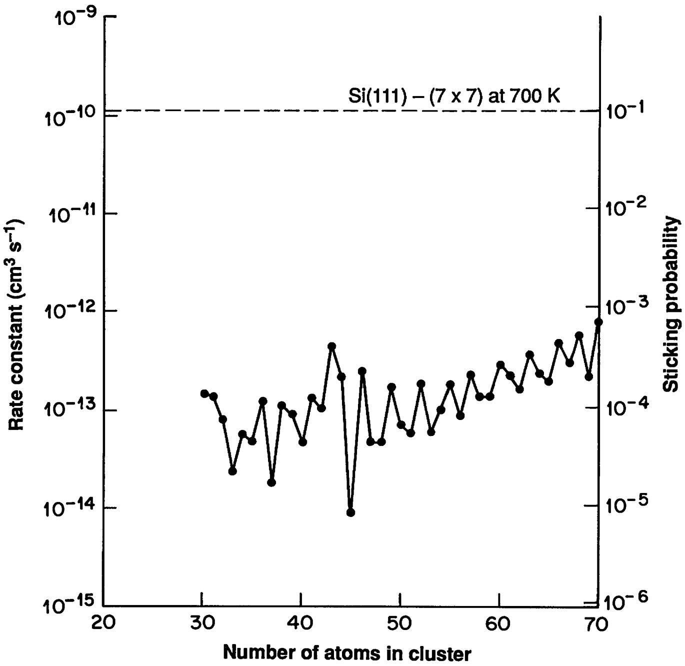

Fig. 7. Rate constants for dissociative chemisorption of ammonia on size-selected silicon cluster ions at 700 K [data from (*13*)]. The dashed line shows the reactivity of the Si(111)-(7×7) surface toward ammonia at 700 K (*34*).

Saturation Studies

Most of the chemical reactions described above result in a series of products of the general form $Si_n(\text{reagent})_m^+$. The experiments described up to this point have been directed mainly at determining the sticking probability of the first reagent molecule onto the cluster. Another question we might ask is: how many reagent molecules will adsorb if the cluster is exposed to an excess of reagent and given plenty of time to react? Saturation studies can provide valuable information on the number and nature of the reactive sites, and the structure of the products (*39*). The reactions with ammonia occur very rapidly at room temperature, and saturation experiments yield some intriguing results (*13*).

Figure 8 shows plots of the average number of ammonia molecules adsorbed on Si_{20}^+ and Si_{40}^+ against ammonia pressure in the drift tube. As a rough calibration, at 0.1 mtorr the clusters are exposed to around ten collisions with ammonia. With this low exposure Si_{20}^+ adsorbs an average of three ammonia molecules and Si_{40}^+ adsorbs four. As the ammonia pressure is increased by over three orders of magnitude, however, the average number of adsorbed ammonia molecules increases only very slowly. Nearly all the atoms in Si_{40}^+ are surface atoms and it is surprising that rapid adsorption of ammonia stops so abruptly after the adsorption of so few ammonia molecules. One possible explanation for this observation is that there are only a few special sites on the cluster where molecular adsorption of ammonia is favorable.

Deposited Clusters

Because gas phase silicon clusters with up to 70 atoms are much less reactive than bulk silicon an obvious question is will they retain these properties when they are deposited? Using surface science

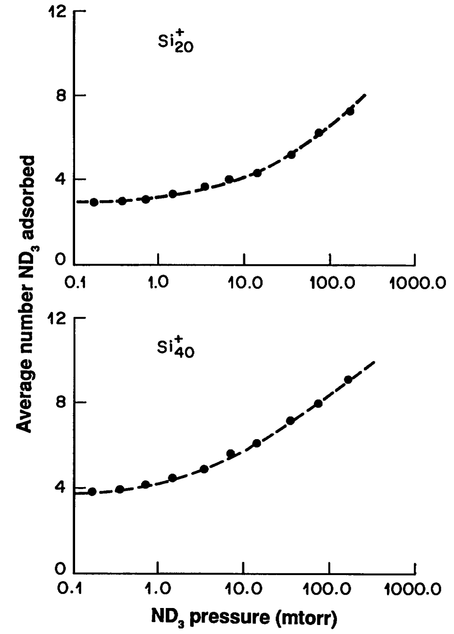

Fig. 8. Plot of the average number of ammonia molecules adsorbed as a function of ammonia pressure for Si_{20}^+ and Si_{40}^+ [data from (*13*)]. As a rough guide a pressure of 0.1 mtorr corresponds to an exposure to around ten collisions with ammonia.

techniques we can investigate the properties of deposited clusters as the coverage is increased from isolated clusters on the surface to a thin film of cluster-assembled material. These experiments, however, are extremely difficult and must be performed under ultrahigh vacuum conditions just like any other surface science experiment. Some of the results of these studies were mentioned above, where it was pointed out that, unlike the gas phase clusters, Si_{10} clusters deposited on amorphous carbon do not undergo etching reactions. To investigate the chemical properties of deposited clusters they are exposed to a known amount of reagent and x-ray photoelectron spectroscopy (XPS) is used to determine the amount of reagent adsorbed (*21*). Measurements of the initial sticking coefficient of oxygen on deposited silicon clusters with around 50 atoms indicate that it is close to that of the clusters in the gas phase and considerably smaller than the sticking coefficient on bulk silicon, even for cluster coverages of around a monolayer. Thus it appears that deposited clusters are just as unreactive as gas phase clusters.

Why Are the Clusters So Unreactive?

A rather consistent picture has emerged from these studies. Silicon clusters with up to 70 atoms, in the gas phase or deposited, appear to be much less reactive than bulk silicon surfaces. With metal clusters, bulk-like chemical behavior is approached for much smaller clusters. Recent studies of the adsorption of carbon monoxide on small copper cluster ions show that bulk behavior occurs with as few as eight atoms (*40*). In other studies it appears that more atoms are required, but 25 atoms appear to be enough for bulk-like chemical behavior to emerge for a metal cluster (*4*).

It is unlikely that the low reactivity of the clusters arises because they are charged (this certainly could not account for the low reactivity of the deposited clusters since they are neutralized). Numerous studies of the reactions of positive ions have shown that they usually proceed more rapidly than the corresponding neutral reactions because the ion-induced dipole interaction lowers the energy of activation barriers. Kaldor and co-workers (*41*) have investigated the influence of charge on the chemical reactivity of metal clusters. For clusters with $n > 25$ (where cluster size effects on reactivity have diminished) the reaction rates for the charged clusters were either approximately the same (Nb_n) or larger (Fe_n) than for the corresponding neutrals.

Recent studies of the reactions of oxygen, water, and ammonia (*17, 25, 34–36*) with bulk silicon have shown that dangling bond sites play a crucial role in dissociative chemisorption of these reagents. Blocking the dangling bond sites inhibits the reactions. So the most reasonable explanation for the low reactivity of the silicon clusters compared to the bulk surfaces is that the clusters have a lower dangling bond density. This would occur if clusters with up to 70 atoms have compact structures similar to those predicted for the smaller clusters. The notion that these clusters have compact high coordination number structures can also account for the observation that all of the larger clusters (not just a few special ones) are much less reactive than the bulk. It is worth noting that the energy difference between the more compact β-tin structure and the diamond structure of bulk silicon is only 0.2 to 0.3 eV per atom (*42*), which is comparable to the energy difference between the (2×1) and (7×7) reconstructions of the Si(111) surface (~0.17 eV per atom) (*43*). The majority of the atoms are surface atoms even with a 70-atom cluster, so it is not unreasonable that these large clusters will adopt compact, low surface energy structures, even at the expense of slightly less favorable bonding for the interior atoms.

Conclusions and Outlook

Studies of the physical and chemical properties of size-selected clusters continue to reveal unexpected behavior, and provide insight into the development of bulk properties. This article has focused on studies of the chemical properties of size-selected silicon clusters. While the chemical reactions that occur on the nanosurfaces of these clusters show obvious qualitative similarities to the processes that occur on bulk silicon surfaces, clusters with up to 70 atoms are much less reactive than bulk silicon surfaces. Cluster structure has emerged as a key issue in these studies. Structural isomers react with some reagents (but not all) with significantly different rates. Annealing the clusters can alter the relative abundances of the reactive and unreactive isomers. And finally the low reactivity observed even for the silicon clusters with up to 70 atoms shows that they are not just small crystals of bulk silicon, but suggests they have reconstructed to more compact structures. Clearly, the next challenge is to develop experimental techniques that can directly probe the structure of these small clusters of atoms.

REFERENCES AND NOTES

1. See, for example, A. W. Castleman and R. G. Keesee, *Science* **241**, 36 (1988); M. A. Duncan and D. H. Rouvray, *Sci. Am.* **261**, 110 (December 1989); Proceedings of Faraday Symposium 25 on Large Gas Phase Clusters, *J. Chem. Soc. Faraday Trans.* **86**, 2343 (1990); Proceedings of the Fifth International Symposium on Small Particles and Inorganic Clusters, *Z. Phys. D*, in press.
2. W. D. Knight *et al.*, *Phys. Rev. Lett.* **52**, 2141 (1984).
3. W. A. de Heer *et al.*, *ibid.* **59**, 1805 (1987); C. R. C. Wang, S. Pollack, D. Cameron, M. M. Kappes, *J. Chem. Phys.* **93**, 3787 (1990); V. Bonacic-Koutecky, P. Fantucci, J. Koutecky, *ibid.*, p. 3802.
4. For examples of recent experimental studies of the chemical properties of atomic clusters see, E. K. Parks *et al.*, *J. Chem. Phys.* **88**, 1622 (1988); D. M. Cox, K. C. Reichmann, D. J. Trevor, A. Kaldor, *ibid.*, p. 111; L. Song and M. A. El-Sayed, *J. Phys. Chem.* **914**, 7907 (1990); Y. Hamrick *et al.*, *J. Chem. Phys.* **88**, 4095 (1988); S. W. Buckner, J. R. Gord, B. S. Freiser, *ibid.*, p. 3678; M. L. Mandich, V. E. Bondybey, W. D. Reents, *ibid.* **86**, 4245 (1987); S. W. McElvany, *ibid.* **89**, 2063 (1988); S. K. Loh, L. Lian, P. B. Armentrout, *ibid.* **91**, 6148 (1989); S. A. Ruatta, L. Hanley, S. L. Anderson, *ibid.*, p. 226.
5. For examples of recent theoretical studies of silicon clusters see, G. Pacchioni and J. Koutecky, *J. Chem. Phys.* **84**, 3301 (1986); R. Biswas and D. R. Hamann, *Phys. Rev. B* **34**, 895 (1986); D. Tomanek and M. Schluter, *ibid.* **36**, 1208 (1987); D. A. Jelski, Z. C. Wu., T. F. George, *Chem. Phys. Lett.* **150**, 447 (1988); P. Ballone, W. Andreoni, R. Carr, M. Parrinello, *Phys. Rev. Lett.* **60**, 271 (1988); H.-X. Wang and R. P. Messmer, *Phys. Rev. B* **41**, 5306 (1990); J. R. Chelikowsky and J. C. Phillips, *Phys. Rev. Lett.* **63**, 1653 (1989); E. Kaxiras, *ibid.* **64**, 551 (1990); K. Raghavachari and C. M. Rohlfing, *J. Chem. Phys.* **89**, 2219 (1988).
6. For a review of the recent theoretical work see, K. Raghavachari, *Phase Trans.* **24–26**, 61 (1990).
7. M. F. Jarrold, J. E. Bower, K. M. Creegan, *J. Chem. Phys.* **90**, 3615 (1989).
8. T. G. Dietz, M. A. Duncan, R. E. Smalley, *ibid.* **74**, 6511 (1981); V. E. Bondybey and J. H. English, *ibid.*, p. 6978.
9. K. M. Creegan and M. F. Jarrold, *J. Am. Chem. Soc.* **112**, 3768 (1990).
10. S. Maruyama, L. R. Anderson, R. E. Smalley, *J. Chem. Phys.* **93**, 5249 (1990).
11. M. F. Jarrold, U. Ray, Y. Ijiri, *Z. Phys. D*, in press.
12. L. A. Bloomfield, R. R. Freeman, W. L. Brown, *Phys. Rev. Lett.* **54**, 2246 (1985); W. Begemann, K. H. Meiwes-Broer, H. O. Lutz, *ibid.* **56**, 2248 (1986); Q.-L. Zhang, Y. Liu, R. F. Curl, F. K. Tittel, R. E. Smalley, *J. Chem. Phys.* **88**, 1670 (1988); M. F. Jarrold and J. E. Bower, *J. Phys. Chem.* **92**, 5702 (1988).
13. M. F. Jarrold, Y. Ijiri, U. Ray, *J. Chem. Phys.*, in press.
14. J. Yoshinobu, H. Tsuda, M. Onchi, M. Nishijima, *ibid.* **87**, 7332 (1988); J. Yoshinobu, H. Tsuda, M. Onchi, M. Nishijima, *Solid State Commun.* **60**, 801 (1986); M. N. Piancastelli *et al.*, *Phys. Rev. B* **35**, 1461 (1987).
15. M. F. Jarrold, U. Ray, K. M. Creegan, *J. Chem. Phys.* **93**, 224 (1990).
16. W. R. Creasy, A. O'Keefe, J. R. McDonald, *J. Phys. Chem.* **91**, 2848 (1987).
17. P. Gupta, C. H. Mak, P. A. Coon, S. M. George, *Phys. Rev. B* **40**, 7739 (1989).
18. P. Morgen, W. Wurth, E. Umbach, *Surf. Sci.* **152**, 1086 (1985).
19. P. E. Wierenga, M. J. Sparnaay, A. van Silfhout, *ibid.* **99**, 56 (1980); H. Ibach, H. D. Bruchmann, H. Wagner, *App. Phys. A* **29**, 113 (1982); E. G. Michel *et al.*, *Phys. Rev. B* **38**, 13399 (1988); W. C. M. Claassen, R. W. A. H. Schmitz, J. Dieleman, *Surf. Sci.* **36**, 240 (1989); M. L. Yu and B. N. Eldridge, *Phys. Rev. Lett.* **58**, 1691 (1987); M. P. D'Evelyn, M. N. Nelson, T. Engel, *Surf. Sci.* **186**, 75 (1987); W. Ranke and Y. R. Xing, *ibid.* **157**, 353 (1985); C. Silvestre and M. Shayegan, *Phys. Rev. B* **37**, 10432 (1988); U. Memmert and M. L. Yu, *Chem. Phys. Lett.* **164**, 552 (1989).
20. H. Ibach, K. Horn, R. Dorn, H. Luth, *Surf. Sci.* **38**, 433 (1973); N. Kasupke and M. Henzler, *ibid.* **92**, 407 (1980).
21. J. E. Bower and M. F. Jarrold, in preparation.
22. U. Ray, M. F. Jarrold, K. M. Creegan, J. E. Bower, *Int. J. Mass Spectrom. Ion Proc.* **100**, 625 (1990).

23. U. Ray and M. F. Jarrold, *J. Chem. Phys.*, in press.
24. H. Ibach, H. Wagner, D. Bruchmann, *Solid State Commun.* **42**, 457 (1982).
25. B. G. Koehler, C. H. Mak, S. M. George, *Surf. Sci.* **221**, 565 (1989).
26. P. Gupta, C. H. Mak, P. A. Coon, S. M. George, in preparation.
27. J. A. Schaefer, J. Anderson, G. J. Lapeyre, *J. Vac. Sci. Technol. A* **3**, 1443 (1985); D. Schmeisser and J. E. Demuth, *Phys. Rev. B* **33**, 4233 (1986); M. Nishijima, K. Edamoto, Y. Kubota, S. Tanaka, M. Onchi, *J. Chem. Phys.* **84**, 6458 (1986); K. Fujiwara, *Surf. Sci.* **108**, 124 (1981); R. A. Rosenberg, P. J. Love, V. Rehn, *J. Vac. Sci. Technol. A* **4**, 1451 (1986); Y. J. Chabal, *Phys. Rev. B* **29**, 3677 (1984); W. Ranke and Y. R. Xing, *Surf. Sci.* **157**, 339 (1985).
28. J. R. Chelikowsky and J. C. Phillips, *Phys. Rev. B* **41**, 5735 (1990).
29. O. Echt, K. Sattler, E. Recknagel, *Phys. Rev. Lett.* **47**, 1121 (1981).
30. T. Su and M. T. Bowers, in *Gas Phase Ion Chemistry*, M. T. Bowers, Ed. (Academic Press, New York, 1979), vol. 1.
31. U. Ray and M. F. Jarrold, in preparation.
32. M. F. Jarrold and J. E. Bower, *J. Am. Chem. Soc.* **111**, 1979 (1989).
33. U. Ray and M. F. Jarrold, *J. Chem. Phys.* **93**, 5709 (1990).
34. B. G. Koehler, P. A. Coon, S. M. George, *J. Vac. Sci. Technol. B* **7**, 1303 (1989).
35. R. Wolkow and Ph. Avouris, *Phys. Rev. Lett.* **60**, 1049 (1988); Ph. Avouris, F. Bozso, R. J. Hamers, *J. Vac. Sci. Technol. B* **5**, 1387 (1987); R. J. Hamers, Ph. Avouris, F. Bozso, *Phys. Rev. Lett.* **59**, 2071 (1987).
36. F. Bozso and Ph. Avouris, *Phys. Rev. B* **38**, 3937 (1988); *Phys. Rev. Lett.* **57**, 1185 (1986).
37. K. Raghavachari, J. Chandrasekhar, M. S. Gordon, K. J. Dykema, *J. Am. Chem. Soc.* **106**, 5853 (1984).
38. J. L. Elkind, J. M. Alford, F. D. Weiss, R. T. Laaksonen, R. E. Smalley, *J. Chem. Phys.* **87**, 2397 (1987); J. M. Alford and R. E. Smalley, *Mat. Res. Soc. Symp. Proc.* **131**, 3 (1989).
39. E. K. Parks, K. Liu, S. C. Richtsmeier, L. G. Pobo, S. J. Riley, *J. Chem. Phys.* **82**, 5470 (1985); T. D. Klots, B. J. Winter, E. K. Parks, S. J. Riley, *ibid.* **92**, 2110 (1990).
40. R. E. Leuchtner, A. C. Harms, A. W. Castleman, *ibid.*, p. 6527.
41. M. R. Zakin, R. O. Brickman, D. M. Cox, A. Kaldor, *ibid.* **88**, 3555 (1988); M. R. Zakin, R. O. Brickman, D. M. Cox, A Kaldor, *ibid.*, p. 6605.
42. M. T. Yin and M. L. Cohen, *Phys. Rev. B* **26**, 5668 (1982).
43. P. Badziag and W. S. Verwoerd, *ibid.* **40**, 1023 (1989).
44. The work described in this article was performed in collaboration with J. E. Bower, K. M. Creegan, U. Ray, and Y. Ijiri.

1990: Annus Mirabilis of Potassium Channels

CHRISTOPHER MILLER

Voltage-gated potassium channels make up a large molecular family of integral membrane proteins that are fundamentally involved in the generation of bioelectric signals such as nerve impulses. These proteins span the cell membrane, forming potassium-selective pores that are rapidly switched open or closed by changes in membrane voltage. After the cloning of the first potassium channel over 3 years ago, recombinant DNA manipulation of potassium channel genes is now leading to a molecular understanding of potassium channel behavior. During the past year, functional domains responsible for channel gating and potassium selectivity have been identified, and detailed structural pictures underlying these functions are beginning to emerge.

WE DO NOT UNDERSTAND HOW WE THINK, BUT WE DO know that the electrical signals passed around the thinking brain are generated by a single class of protein: the ion channels. In contrast to electrical signals in computers, which are carried by electrons flowing longitudinally along wires, bioelectric impulses are generated by charges flowing transversely across the thin membranes covering cells. In nerve cells, the charges are carried by the biologically abundant inorganic ions, Na^+, K^+, Ca^{2+}, and Cl^-; the ion channel proteins catalyze this transmembrane flow of ionic charge. They do this in a simple way: by forming narrow, hydrophilic pores through which ions can diffuse passively (*1*).

To operate sensibly, ion channels must perform two essential tasks. First, they must open or close rapidly in response to biological signals. A term for this process, reflecting the early influence of electrical engineers, is "gating"; biochemists likewise describe channels as proteins able to switch among conducting and nonconducting conformations. Second, the open pore must faithfully choose which ions will permeate and which will not. Extreme cases are known in which the preferred substrate, K^+, permeates the pore at a rate 10^4-fold higher than the rate for Na^+, which is only 0.4 Å smaller in crystal radius. This is an impressive trick because these ions do not possess the geometrically elaborate structures that allow organic substrates to be recognized so specifically by enzymes. A long-held aim of ion channel research is to understand these two crucial functions—gating and ionic selectivity—in terms of the molecular structures of the channel proteins. In spite of the proliferation of methods for detecting currents through single ion channels, the lack of general approaches for crystallizing membrane proteins has prevented a direct view of the structural underpinnings of their workings.

During the past year, however, a frisson has rippled through the field because for the first time a physical picture underlying basic channel behaviors is beginning to emerge in tantalizing snatches. Much of this excitement surrounds a newcomer to the collection of channels attackable at the molecular level: the family of voltage-gated K^+ channels. These results represent the early fruits of recombinant DNA manipulation, which is just now finding wide application to ion channel genes. These approaches have provided structural conclusions about K^+ channels on three issues about which classical electrophysiology has been silent: the precise nature of the conformational changes underlying voltage-dependent gating, the molecular makeup of the ion conduction pathway, and the oligomeric state of the functional channel. Each of these experimental efforts has opened a qualitatively new window on the molecular black box of K^+ channels and of voltage-dependent ion channels in general.

Shaker: The Big Break

The new results on K^+ channels were made possible by the molecular cloning of the *shaker* gene of *Drosophila* (*2*). This gene codes for a voltage-dependent K^+ channel, or rather for a multiplic-

---

The author is in the Howard Hughes Medical Institute, Graduate Department of Biochemistry, Brandeis University, Waltham, MA 02254.